# INVESTIGATIONS IN SINGLE LAYER GRAVITATIONAL POTENTIAL

A Thesis by

Darrell Anne Stewart

Bachelor of Arts, University of North Carolina Asheville, 1995

Master of Arts, California State University Fullerton, 2005

Submitted to the Department of Mathematics and Statistics
and the faculty of the Graduate School of
Wichita State University
in partial fulfillment of
the requirements for the degree of
Master of Science

May 2010

**INVESTIGATIONS IN SINGLE LAYER GRAVITATIONAL POTENTIAL**

The following faculty members have examined the final copy of this thesis for form and content, and recommend that it be accepted in partial fulfillment of the requirement for the degree of Master of Science with a major in Applied Mathematics.

Victor Isakov, Committee Chair

Tom DeLillo, Committee Member

Yanwu Ding, Committee Member

## TABLE OF CONTENTS

**Chapter** **Page**

## LIST OF TABLES

**Table** **Page**

## LIST OF FIGURES

**Figure** **Page**

# CHAPTER 1

# Introduction

## 1.1 Single layer potential

The gravitational potential generated by a mass distribution $\mu$ in $\mathbb{R}^n$ is

$$U(\mathbf{x};\mu) = \int K(\mathbf{x},\mathbf{y})d\mu(\mathbf{y}), \tag{1.1.1}$$

where

$$K(\mathbf{x},\mathbf{y}) = \begin{cases} -\frac{1}{2\pi}\ln|\mathbf{x}-\mathbf{y}|, & n=2, \\ 1/4\pi|\mathbf{x}-\mathbf{y}|, & n=3. \end{cases} \tag{1.1.2}$$

Let $D$ be an open bounded set, $D \subset \Omega \subset \mathbb{R}^n$ where $\Omega$ is given and open. The inverse problem of gravimetry is to find $\mu$ given $U(;\mu)$ outside $\Omega$. We will assume that $D$ is convex, $\mu$ is zero outside $\bar{D}$, and that $\mu$ is a characteristic function of $D$, $\mu = \chi_D$. Under these conditions we know from [2] that if we are given $u$ outside $\Omega$, then we can solve for $\mu$ and $\mu$ is unique. Gravitational potential can also be written in single layer representation and we represent our problem by

$$\partial^\alpha u(\mathbf{x}; gd\Gamma) = \int_{\partial\Omega} \partial^\alpha K(\mathbf{x},\mathbf{y})g(\mathbf{y})d\Omega(\mathbf{y}), \mathbf{x} \in \partial\Omega. \tag{1.1.3}$$

where $\partial^\alpha u$ represents the derivatives of $u$, $\partial/\partial x_\alpha$ with $\alpha = 1,2,3$, $\Gamma = \partial\Omega$, and $g(\mathbf{y})$ is the density of which the potential is distributed over $\Gamma$. For this paper we study the Cauchy problem where we are given $\partial^\alpha u(\mathbf{x}; gd\Gamma)$ in $\mathbb{R}^n \setminus \overline{\Omega}^- = \Omega^+$ and we solve for $g(\mathbf{y})$ on $\Gamma$. Following the findings in [1], we will assume $\Gamma \in C^{1+\lambda}$ and $u \in H^{2,2}$ so that $g \in L^2(\Omega)$.

## 1.2 Properties of Single Layer Potentials

First we study the regularity properties needed to take derivatives and the jump relations needed to handle where the integral becomes singular on $\Gamma$. Let $\alpha = 0$ and consider the single layer potential

$$u(\mathbf{x}; gd\Omega) = \int_{\partial\Omega} K(\mathbf{x},\mathbf{y})g(\mathbf{y})d\Omega(\mathbf{y}), \mathbf{x} \in \partial\Omega. \tag{1.2.1}$$

and the Newtonian potential

$$U(\mathbf{x}; f) = \int K(x, y) f(y) dy. \tag{1.2.2}$$

### 1.2.1 Preliminaries

We state seleceted definitions and theorems found in [1] that will be needed to justify our properties.

**Definition 1.2.1.** A real or complex valued funciton $\phi$ defined on a set $\Omega \subset \mathbb{R}^m$ is called uniformly Hölder continuous with Hölder exponent $0 < \lambda \leq 1$, if there exists a constant $C$ such that

$$|\phi(\mathbf{x}) - \phi(\mathbf{y})| \leq C|\mathbf{x} - \mathbf{y}|^\lambda \tag{1.2.3}$$

for all $\mathbf{x}, \mathbf{y} \in \Omega$. By $C^{k,\alpha}(\overline{\Omega})$ we denote the linear space of all functions defined on $\Omega$ which are bounded, uniformly Hölder continuous with exponent $\lambda$, and have derivatives up to order integer $k > 0$ which are also uniformly Hölder continuous. The space $C^{k,\alpha}(\overline{\Omega})$ is called a Hölder space.

Note that a second order linear differential operator $A$ with real-valued coefficients $a^{jk}$, $a^j$, $a \in C(\overline{\Omega})$ will be considered. A classical solution to the equation $Au = 0$ in $\Omega$ is a function $u \in C^2(\Omega)$ satisfying this equation in $\Omega$.

**Theorem 1.2.1** (Maximum principles)**.** *Suppose $u$ is a classical solution to the equation $Au = f$ (where $A$ is a second-order linear differential operator) on a domain $\Omega$ with $a \geq 0$ and $f \geq 0$ on $\Omega$.*

*i) (Hopf's) If $u$ takes its nonpositive minimum over $\Omega$ at a point of $\Omega$ then $u$ is constant on $\Omega$.*

*ii) (Giraud's) Suppose that a hypersurface $\Gamma \in C^{1+\lambda}$ is part of $\partial\Omega$ and $\mathbf{l}$ is a unit vector with $\langle \mathbf{l}, \mathbf{n} \rangle > 0$ where $\mathbf{n}$ is a normal at $x \in \Gamma$ exterior with respect to $\Omega$. If a classical solution $u$ has a continuous continuation on to $\Omega \cup x$ and takes its nonpositive minimum over $\Omega \cup x$ at $x$ then either $u$ is constant on $\Omega$ or there is $\epsilon > 0$ such that $u(x - t\mathbf{l}) - u(x) > \epsilon t$ for $0 < t < \epsilon$.*

From Hopf's principle we can conclude that any nonconstant solution to the equation $Au = 0$ with $a > 0$ cannot take its extremum on $\Omega$.

**Corollary 1.2.1.** If in addition to the conditions on Giraud's principle of 1.2.1 there is the derivative $\partial u/\partial \mathbf{l}(x)$ and $u$ is not constant then $\partial u/\partial \mathbf{l}(x) < 0$.

### 1.2.2 Regularity, Real Case

As found in [1], we have the following regularity properties of single layer potential.

**Theorem 1.2.2** (Regularity)**.**

**Theorem 1.2.3** (Higher-order Regularity)**.** *Let $k - \{k\} > 0$ and $\Gamma_1 = \Gamma \cap V$, $\Omega_1 = \Omega \cap V$ where $V$ is an open set. If $\Gamma_1 \in C^{k+1}$ (is analytic), $g \in C^k(\Gamma_1)$, and the coefficients of $A$ belong to $C^k(\Omega_1)$ (are analytic related sets) then $u^{\pm} \in C^{k+1}(\Omega_1 \cup \Gamma_1)$ (is analytic on $\Omega_1^{\pm}$ and analytically continuable across $\Gamma_1$).*

### 1.2.3 Regularity, Complex Case

From [3] we have the same results in the complex case that correspond to the real case $\mathbb{R}^2$. Let $\Omega$ be a bounded and simply connected domain in the complex plane. We assume $\partial\Omega \in C^2$ and the normal vector $\nu$ is directed into the exterior of $\Omega$. Complex integration along $\partial\Omega$ is in the counterclockwise direction. The single layer potential is given by

$$u(z) := \frac{1}{2\pi} \int_{\partial\Omega} g(\zeta) \log \frac{1}{|\zeta - z|} ds(\zeta), z \in \mathbb{C} \setminus \partial\Omega. \tag{1.2.4}$$

We can employ the connection between two-dimensional harmonic functions and holomorphic functions to develop regularity for the single layer potential in the complex case by using the Sokhotski-Plemelj Theorem.

**Theorem 1.2.4.** *(Sokhotski-Plemelj) For densities $g \in C^{0,\lambda}(\partial\Omega)$ the holomorphic function $f$ defined by the Cauchy integral*

$$f(z) := \frac{1}{2\pi i} \int_{\partial\Omega} \frac{\phi(\zeta)}{\zeta - z} d\zeta, z \in \mathbb{C} \setminus \partial\Omega, \tag{1.2.5}$$

*can be uniformly Hölder continuously extended from* $\Omega$ *into* $\overline{\Omega}$ *and from* $\mathbb{C}\setminus\overline{\Omega}$ *into* $\mathbb{C}\setminus\overline{\Omega}$ *with limiting values*

$$f_{\pm}(z) = \frac{1}{2\pi i}\int_{\partial\Omega}\frac{g(\zeta)}{\zeta - z}d\zeta \mp \frac{1}{2}g(z), z \in \partial\Omega. \tag{1.2.6}$$

*where* $f_{\pm}(z) = \lim_{h\to+0} f(z \pm hr(z))$. *Also, inequalities* $\|f\|_{\lambda,\overline{\Omega}^+} \leq C\|g\|_{\lambda}$, $\|f\|_{\lambda,\overline{\Omega}^-} \leq C\|g\|_{\lambda}$ *for some* $C$ *depending on* $\lambda$ *and* $\partial\Omega$.

We know that complex integration and contour integration along $\partial\Omega$ is related by

$$dz = e^{i\gamma(z)}ds(z) \tag{1.2.7}$$

for all $z \in \partial\Omega$ where $\gamma(z)$ denotes the angle between the tangent to $\partial\Omega$ at the point $z$ and the real axis. Since $\partial\Omega$ is of class $C^2$ this angle is continuously differentiable with respect to $z$. Therefore, from Theorem 1.2.4 we see that the Cauchy Integral (1.2.5) is holomorphic in $\Omega$ and $\mathbb{C}\setminus\Omega$ and can be uniformly Hölder continuously extended from $\Omega$ into $\overline{\Omega^+}$ and from $\mathbb{C}\setminus\overline{\Omega}$ into $\mathbb{C}\setminus\Omega$ with limiting values

$$f_{\pm}(z) = \frac{1}{2\pi}\int_{\partial\Omega}\frac{g(\zeta)}{\zeta - z}ds(\zeta) \mp \frac{i}{2\pi}e^{-i\gamma(z)}g(z), z \in \partial\Omega. \tag{1.2.8}$$

The gradient of the logarithmic single-layer potential (1.2.4) is given by

$$\nabla u(z) = \frac{1}{2\pi}\int_{\partial\Omega} g(\zeta)\frac{\zeta - z}{|\zeta - z|^2}ds(\zeta), z \in \mathbb{C}\setminus\partial\Omega. \tag{1.2.9}$$

Notice that (1.2.9) is the complex conjugate of the holomorphic function $f$ given by the Cauchy integral (1.2.5) and the complex conjugate of $-ie^{-i\gamma(z)}$ corresponds to the normal $\nu(z)$ at $z \in \partial\Omega$. So by Theorem 1.2.4 we have the following theorem.

**Theorem 1.2.5.** *The first derivatives of the logarithmic single-layer potential* $u$ *with Hölder continuous density can be extended uniformly Hölder continuously from* $\Omega$ *into* $\overline{\Omega}$ *and from* $\mathbb{C}\setminus\overline{\Omega}$ *into* $\mathbb{C}\setminus\Omega$ *with limiting values*

$$\nabla u_{\pm}(z) = \frac{1}{2\pi}\int_{\partial\Omega} g(\zeta)\nabla\log\frac{1}{|\zeta - z|}ds(\zeta) \mp \frac{1}{2}\nu(z)g(z), z \in \partial\Omega. \tag{1.2.10}$$

### 1.2.4 Jump relations

The analysis of boundary value problems require the following properties of these potentials for points $\mathbf{x} \in \partial\Omega$ since the integral becomes singular at these points.

**Theorem 1.2.6** (Jump Relations)**.** *If $g \in C(\partial\Omega)$, then for all $x \in \partial\Omega$ there are*

$$(\partial/\partial\nu)u^{\pm}(x) = \mp\frac{1}{2}g(x) + (\partial/\partial\nu)u(x; gd\Omega). \tag{1.2.11}$$

### 1.2.5 Other Remarks

Let $u$ be the single layer potential as in 1.2.1 and $U = U(; f_\chi(\Omega^-)$ be the Newtonian potential as in 1.2.2, $f \in L_\infty(\Omega^-)$. Then from Theorems 1.2.2 and 1.2.6 we see that for $g \in C(\partial\Omega)$ we have

$$Au^{\pm} = 0, \tag{1.2.12}$$

$$u^+ = u^- on \partial\Omega, \tag{1.2.13}$$

and

$$(\partial/\partial\nu)u^- - (\partial/\partial\nu)u^+ = g \quad \text{on } \partial\Omega. \tag{1.2.14}$$

Also,

$$AU^{\pm} = 0, \tag{1.2.15}$$

$$U^+ = U^- on \partial\Omega, \tag{1.2.16}$$

and

$$(\partial/\partial\nu)U^+ = (\partial/\partial\nu)U^- \quad \text{on } \partial\Omega. \tag{1.2.17}$$

If K is a Green's function then

$$\lim U^+(x) = \lim u^+ = 0 as |x| \to +\infty. \tag{1.2.18}$$

If $A = -\Delta$, $\Omega \subset \mathbb{R}^2$, and $K$ is the logarithmic kernel, then we have

$$U^+(x; \mu) = C \ln|x| + U_0^+(x) \tag{1.2.19}$$

where $U_0^+(x) \to 0$ as $|x| \to \infty$.

A measure $u$ on $\mathbb{R}^n$ is said to be a (generalized, or distribution) solution to the equation $Au = \mu$ on $\mathbb{R}^n$ if

$$u(A^t\phi) = \mu(\phi) \tag{1.2.20}$$

for all $\phi \in C_0^\infty(\mathbb{R}^n)$. If u has the density $u(x)$ (with respect to the Lebesgue measure $dx$) the the definition is equivalent to

$$\int u(x)A^t\phi(x)dx = \int \phi d\mu \tag{1.2.21}$$

for all $\phi \in C_0^\infty(\mathbb{R}^n)$.

**Theorem 1.2.7.** *Let $S$ be a compact subset of $\mathbb{R}^n$ and $supp\mu \subset S$. If $Au = \mu$ on $\mathbb{R}^n$ and $u = 0$ on $\mathbb{R}^n \setminus S$ then*

$$\int v d\mu = 0 \tag{1.2.22}$$

*for all solutions to the equation $A^tv = 0$ on neighborhoods of $S$.*

*Proof.* According to 1.2.21 we have

$$\int u(x)A^t\phi(x)dx = \int \phi d\mu \tag{1.2.23}$$

for any $\phi \in C_0^2(\mathbb{R}^n)$. Since $u = 0$ and $\mu = 0$ on $\mathbb{R}^n \setminus S$ this relation is valid for any function $\phi \in C^2(V(S))$. Due to the regularity of distributions solutions of elliptic equations, any solution to $A^tv = 0$ on $V(S)$ belongs to $C^2(V(S))$. Let $\phi = v$ and the proof is complete. □

**Theorem 1.2.8.** *Suppose $\Omega^-$ is a bounded domain of class $C^{1+\lambda}$ with $\overline{\Omega}^- \subset \mathbb{R}^2$, $\partial\Omega = \Gamma$, and $\Delta U^+ = 0$ on $\Omega^+$ (where $\Omega^+ := \mathbb{R}^2 \setminus \overline{\Omega}^-$), $U^+ \in C^1(\Omega^+)$. In addition, suppose that $U_0^+(x) \to 0$ as $|x| \to \infty$. Then there is a function $g \in C(\Gamma)$ such that*

$$U^+ = u(; gd\Gamma) \quad \text{on } \mathbb{R}^2 \setminus \overline{\Omega}^-. \tag{1.2.24}$$

*Proof.* Consider Fredholm integral equation from 1.2.11

$$(\partial/\partial\nu)u^+(x) = -\frac{1}{2}g(x) + (\partial/\partial\nu)u(x; gd\Gamma) \quad \text{on } \Gamma. \tag{1.2.25}$$

We need to show that this equation has a unique solution $g \in C(\Gamma)$. It is sufficient to prove that the related homogeneous problem with $g = 0$ has only the zero solution. Then we have

$$(\partial/\partial\nu)u^+(x) = (\partial/\partial\nu)u(x; gd\Gamma) \quad \text{on } \Gamma. \tag{1.2.26}$$

Taking this approach we see that $\frac{\partial u^+}{\partial \nu} = 0$ and that $U^+$ behaves as in 1.2.19. Suppose we have $C > 0$ in this relation. Then $U^+$ has a minimum, call it $x_o$, in the region $\overline{\Omega}^+$. If $x_o \in \Omega^+$, then by Hopf's maximum principle of Theorem 1.2.1 $U^+$ is constant. If $x_o \in \Gamma$ then $\partial u^+/\partial\nu(x_o) < 0$, a contradiction. Then by the Giraud corollary 1.2.1 $U^+$ is constant. However, from 1.2.19 we cannot have $U^+$ constant. We reach the same contradition with $C < 0$. Therefore, $C = 0$. A similar argument shows that since $U_0^+ \to 0$ as $|x| \to \infty$ that we must also have $U_0^+ = 0$. We can now say that $U^+ = 0$ is the only possibility and $\partial/\partial\nu U^+ = 0$. From the jump relations we see that we must also have $g = 0$. Since the equation is Fredholm, uniqueness implies the existence of $g \in C(\Gamma)$. We conclude that $U^+ = u(; gd\Gamma)$ on $\Omega^+$ since their normal derivatives are equal on $\partial\Gamma$. □

**Theorem 1.2.9.** *If textsupp$\mu \subset \Omega^-$, then there is a function $g \in C(\Gamma)$ such that*

$$U(;\mu) = u(; gd\Gamma) \quad \text{on } \Omega^+. \tag{1.2.27}$$

*If $0 \le \mu$, then $0 \le g$ on $\Gamma$.*

*Proof.* From the condition *supp*$\mu \subset \Omega^-$ it follows that the function $U(;\mu)$ all the conditions of satisfies all the conditions of Theorem 1.2.8; so the existence of $g$ is a consequence of this theorem. From equality 1.2.27 we have

$$\int v d\mu = \int_\Gamma v g d\Gamma \tag{1.2.28}$$

for solutions to the equation $A^t v = 0$ near $\overline{\Omega}^-$. Let $\phi \in C(\Gamma)$ and $0 \le \phi$. Let $v_k$ be solutions to the equation $A^t v = 0$ near $\overline{\Omega}^-$. We may assume a continuous extension of $\phi$ onto $\mathbb{R}^n$ is nonnegative. So, according to the extremum principles, $0 \le v_k$ on $\Omega^-$. Since $\Gamma \in C^{1+\lambda}$ all boundary points of $\Omega^-$ are stability points; so $v_k(x) \to \phi(x)$ for any $x \in \Gamma$. So, using

the positivity of $\mu$ and, as above, passing to the limit in the equality of integrals of $v_k$ with respect to $d\mu$ and $gd\Gamma$ we concluded that

$$\int \phi g d\Gamma \geq 0 \tag{1.2.29}$$

for positive $\phi \in C(\Gamma)$; so $0 \leq g$ on $\Gamma$. $\square$

# CHAPTER 2

## Calculation of Derivatives

This remainder of this paper will focus on gravitational potential in two dimensions. Given the open disk $\Omega = \{\mathbf{y} \in \mathbb{R}^2 : |\mathbf{y}| < R, R > 0\}$, let $u$ be the single-layer gravitational potential generated by $\partial\Omega = \{\mathbf{y} \in \mathbb{R}^2 : |\mathbf{y}| = R\}$. Then for $\mathbf{x} \in \overline{\Omega}^c$ the function $u(\mathbf{x})$ is given by

$$u(\mathbf{x}) = \int_{\partial\Omega} K(\mathbf{x}, \mathbf{y}) g(\mathbf{y})\, d\mathbf{y} \tag{2.0.1}$$

where

$$K(\mathbf{x}, \mathbf{y}) = -\frac{1}{2\pi} \ln |\mathbf{x} - \mathbf{y}|$$

and $g(\mathbf{y})$ is a scalar weight (mass distribution) function.

### 2.1 Real Plane

Given a point mass source with unit density at $y = (y_1, y_2)$, and any other point $x = (x_1, x_2) \neq y$, we have the gravitational potential at $x$ given by

$$u(x) = \ln |x - y|. \tag{2.1.1}$$

The constant $-1/2\pi$ found in the fundamental solution to Laplace's equation is ignored for our purposes. Taking the first partial derivatives with respect to the components of $x$,

$$\partial_{x_1} u(x) = \frac{x_1 - y_1}{|x - y|^2} \tag{2.1.2}$$

and

$$\partial_{x_2} u(x) = \frac{x_2 - y_2}{|x - y|^2}. \tag{2.1.3}$$

Second derivatives are

$$\partial_{x_1} u_{x_1} = \frac{(x_2 - y_2)^2 - (x_1 - y_1)^2}{|x - y|^4}, \tag{2.1.4}$$

$$\partial_{x_2} u_{x_2} = \frac{(x_1 - y_1)^2 - (x_2 - y_2)^2}{|x - y|^4}, \tag{2.1.5}$$

and

$$\partial_{x_2} u_{x_1} = \partial_{x_1} u_{x_2} = \frac{-2(x_1 - y_1)(x_2 - y_2)}{|x - y|^4}. \tag{2.1.6}$$

Note that $u_{x_1 x_1} = -u_{x_2 x_2}$ as would be expected, since $\Delta u = 0$ for any $x \neq y$. The third derivatives are

$$\partial_{x_1} u_{x_1 x_1} = \frac{2(x_1 - y_1)^3 - 6(x_1 - y_1)(x_2 - y_2)^2}{|x - y|^6} = -\partial_{x_1} u_{x_2 x_2} \tag{2.1.7}$$

and

$$\partial_{x_2} u_{x_2 x_2} = \frac{2(x_2 - y_2)^3 - 6(x_2 - y_2)(x_1 - y_1)^2}{|x - y|^6} = -\partial_{x_2} u_{x_1 x_1}. \tag{2.1.8}$$

## 2.2 Complex Plane

Let $T \subset \mathbb{C}$ be a rectangle with $\sigma = \xi + i\eta$ in $R$ (a closed and bounded set) and $s = x + iy$ in the compliment of $T$. Define the potential by

$$\phi(s) := \int_T \rho(\sigma) \ln |s - \sigma| \, dA_\sigma. \tag{2.2.1}$$

Introduce the operator

$$\frac{\partial}{\partial s} = \frac{1}{2}\left(\frac{\partial}{\partial x} - i\frac{\partial}{\partial y}\right) \quad \Rightarrow \quad 2i\frac{\partial}{\partial s} = \left(\frac{\partial}{\partial y} + i\frac{\partial}{\partial x}\right), \tag{2.2.2}$$

and note that

$$\begin{aligned} 2i\frac{\partial}{\partial s} \ln |s - \sigma| &= \left(\frac{\partial}{\partial y} + i\frac{\partial}{\partial x}\right) \frac{1}{2} \ln\left((x - \xi)^2 + (y - \eta)^2\right) \\ &= \frac{(y - \eta) + i(x - \xi)}{|s - \sigma|^2} = i\frac{(x - \xi) - i(y - \eta)}{|s - \sigma|^2} = i\frac{\overline{s - \sigma}}{(s - \sigma)(\overline{s - \sigma})} = \frac{i}{s - \sigma}. \end{aligned} \tag{2.2.3}$$

If $\rho(\sigma) \equiv 2$, then we have

$$G(s) := -2i\frac{\partial}{\partial s}\phi(s) = \left(\frac{\partial}{\partial y} + i\frac{\partial}{\partial x}\right)\phi(s) = 2i\int_T \frac{dA_\sigma}{\sigma - s}. \tag{2.2.4}$$

Using [1, equation (2.5.3), p. 46][1], which we write here as

$$\int_T \frac{1}{\sigma - s} \, dA_\sigma = \int_T \frac{\partial \overline{\sigma}}{\partial \overline{\sigma}} \frac{1}{\sigma - s} \, dA_\sigma = \frac{-i}{2} \int_{\partial T} \frac{\overline{\sigma}}{\sigma - s} \, d\sigma, \tag{2.2.5}$$

[1] Let $F = \overline{\zeta}$ and assume that $\pi F(z)\chi(z;\Omega) \equiv 0$ for the equation in that text.

we can then write

$$G(s) = 2i \int_T \frac{dA_\sigma}{\sigma - s} = \int_{\partial T} \frac{\overline{\sigma}}{\sigma - s}\, d\sigma. \tag{2.2.6}$$

Let $\sigma = \alpha t + \beta$ for $\alpha, \beta \in \mathbb{C}$ and $t \in [t_1, t_2] \subset \mathbb{R}$, with $d\sigma = \alpha dt$, and we have

$$G(s) = \int_{t_1}^{t_2} \frac{|\alpha|^2 t + \alpha\overline{\beta}}{\alpha t + \beta - s}\, dt. \tag{2.2.7}$$

We have also

$$G'(s) = \int_{t_1}^{t_2} \frac{|\alpha|^2 t + \alpha\overline{\beta}}{(\alpha t + \beta - s)^2}\, dt \tag{2.2.8}$$

and

$$G''(s) = 2\int_{t_1}^{t_2} \frac{|\alpha|^2 t + \alpha\overline{\beta}}{(\alpha t + \beta - s)^3}\, dt. \tag{2.2.9}$$

## 2.3 Connection Between Real and Complex Calculations

It should be easy to see from equation (2.2.3) that

$$G(s) = -2i\frac{\partial}{\partial s}\phi(s) \qquad \Rightarrow \qquad u_{x_1} \sim -\mathrm{Im}\left(G(s)\right) \quad \text{and} \quad u_{x_2} \sim -\mathrm{Re}\left(G(s)\right). \tag{2.3.1}$$

The symbol '$\sim$' is used here as 'similar to' to remind ourselves that there are differences between the two representations. In a switch of notation let $s = \alpha + i\beta$. Then

$$\begin{aligned} G'(s) = -\frac{\partial}{\partial s}\left(2i\frac{\partial}{\partial s}\phi(s)\right) &= -\frac{1}{2}\left(\frac{\partial}{\partial \alpha} - i\frac{\partial}{\partial \beta}\right)\left(\frac{\partial}{\partial \beta} + i\frac{\partial}{\partial \alpha}\right)\phi(s) \\ &= -\left[\frac{\partial}{\partial \alpha \partial \beta} + \frac{i}{2}\left(\frac{\partial^2}{\partial \alpha^2} - \frac{\partial^2}{\partial \beta^2}\right)\right]\phi(s). \end{aligned} \tag{2.3.2}$$

So in relation to the potential $u(x)$ we have

$$u_{x_1x_1} - u_{x_2x_2} = 2u_{x_1x_1} \sim -2\mathrm{Im}\left(G'(s)\right) \quad \text{and} \quad u_{x_1x_2} \sim -\mathrm{Re}\left(G'(s)\right). \tag{2.3.3}$$

Taking again the derivative with respect to $s$,

$$\begin{aligned}
G''(s) &= -\frac{\partial}{\partial s}\left[\frac{\partial^2}{\partial\alpha\partial\beta}+\frac{i}{2}\left(\frac{\partial^2}{\partial\alpha^2}-\frac{\partial^2}{\partial\beta^2}\right)\right]\phi(s)\\
&= \frac{1}{2}\left(i\frac{\partial}{\partial\beta}-\frac{\partial}{\partial\alpha}\right)\left[\frac{\partial^2}{\partial\alpha\partial\beta}+\frac{i}{2}\left(\frac{\partial^2}{\partial\alpha^2}-\frac{\partial^2}{\partial\beta^2}\right)\right]\phi(s)\\
&= \frac{1}{2}\left[i\frac{\partial^3}{\partial\alpha\partial\beta^2}-\frac{1}{2}\left(\frac{\partial^3}{\partial\alpha^2\partial\beta}-\frac{\partial^3}{\partial\beta^3}\right)-\frac{\partial^3}{\partial\alpha^2\partial\beta}+\frac{i}{2}\left(-\frac{\partial^3}{\partial\alpha^3}+\frac{\partial^3}{\partial\alpha\partial\beta^2}\right)\right]\phi(s) \quad (2.3.4)\\
&= \frac{1}{2}\left[\frac{1}{2}\frac{\partial^3}{\partial\beta^3}-\frac{3}{2}\frac{\partial^3}{\partial\alpha^2\partial\beta}+i\left(\frac{3}{2}\frac{d^3}{\partial\alpha\partial\beta^2}-\frac{1}{2}\frac{\partial^3}{\partial\alpha^3}\right)\right]\phi(s)\\
&= \frac{1}{4}\left[\frac{\partial^3}{\partial\beta^3}-3\frac{\partial^3}{\partial\alpha^2\partial\beta}+i\left(3\frac{\partial^3}{\partial\alpha\partial\beta^2}-\frac{\partial^3}{\partial\alpha^3}\right)\right]\phi(s).
\end{aligned}$$

The relation to the potential $u(x)$ is then

$$4u_{x_2x_2x_2} = u_{x_2x_2x_2} - 3u_{x_1x_1x_2} \sim 4\mathrm{Re}\left(G''(s)\right) \quad \text{and} \quad -4u_{x_1x_1x_1} = 3u_{x_1x_2x_2} - u_{x_1x_1x_1} \sim 4\mathrm{Im}\left(G''(s)\right). \quad (2.3.5)$$

# CHAPTER 3

## Discretization

If we discretize the problem with $n$ points, say let $\mathbf{y}_j \in \partial\Omega$ and $g_j := g(\mathbf{y}_j)$ where $1 \leq j \leq n$, then the integral 2.0.1 may be approximated by

$$u(\mathbf{x}) \approx \sum_{j=1}^{n} g_j K(\mathbf{x}, \mathbf{y}_j). \tag{3.0.1}$$

We will now consider various types of measurements along a line $\Gamma_0$ of length $L > 0$ located a distance $r$ from $\partial\Omega$. Error will be measured by comparing solutions with the exact potential measured on a disk $\Gamma_{err}$ with radius $\gamma$, where $R < \gamma < r$. So we define

$$\Gamma_0 := \{\mathbf{x} = (x_1, x_2) : -L/2 \leq x_1 \leq L/2, x_2 = r > \gamma\} \tag{3.0.2}$$

and

$$\Gamma_{err} := \{\tilde{\mathbf{x}} = (\tilde{x}_1, \tilde{x}_2) : |\tilde{\mathbf{x}}| = \gamma > R\}. \tag{3.0.3}$$

With measurement points $\mathbf{x}_i \in \Gamma_0$, $1 \leq i \leq n$, let $A := [a_{ij}]$ be a matrix where each entry is given by $a_{ij} := K(\mathbf{x}_i, \mathbf{y}_j)$.

### 3.1 Dirichlet data

If Dirichlet data $f(\mathbf{x}_i) = u(\mathbf{x}_i)$ on $\Gamma_0$ is measured, then we can write $A\mathbf{g} = \mathbf{f}$ and solve for $\mathbf{g}$ as a minimization problem,

$$\min_{\mathbf{g}} \|A\mathbf{g} - \mathbf{f}\|_2.$$

Note that

$$\mathbf{g} := \begin{bmatrix} g_1 \\ \vdots \\ g_n \end{bmatrix} \quad \text{and} \quad \mathbf{f} := \begin{bmatrix} f(\mathbf{x}_1) \\ \vdots \\ f(\mathbf{x}_n) \end{bmatrix}.$$

We calculate the potential for points $\mathbf{x}_i \in \Gamma$ by

$$f(\mathbf{x}_i) = g(\mathbf{a}) \ln |\mathbf{x}_i - \mathbf{a}|, \tag{3.1.1}$$

where $\mathbf{a}$ are points on the boundary of the target region $D$. Let $\hat{f}(\mathbf{x}_i)$ be the measurement data $f$ with noise on the order of $\delta$ added so that

$$\hat{\mathbf{f}} = \begin{bmatrix} \hat{f}(\mathbf{x}_1) & \cdots & \hat{f}(\mathbf{x}_n) \end{bmatrix}^T. \tag{3.1.2}$$

We solve the system $A\mathbf{g} = \hat{\mathbf{f}}$, which gives the mass density $g$ at the points $\mathbf{y}_j \in \partial\Omega$.

To check the accuracy of the solution, we use these mass densities to create the calculated potential at the error measurement points $\tilde{\mathbf{x}}_i \in \Gamma_{err}$ by

$$u(\tilde{\mathbf{x}}_i) = \sum_{j=1}^{n} g(\mathbf{y}_j) \ln |\tilde{\mathbf{x}}_i - \mathbf{y}_j|. \tag{3.1.3}$$

The exact potential at the error measurement points is given by

$$u_{err}(\tilde{\mathbf{x}}_i) = g(\mathbf{a}) \ln |\tilde{\mathbf{x}}_i - \mathbf{a}| = \ln |\tilde{\mathbf{x}}_i - \mathbf{a}|. \tag{3.1.4}$$

Define the vectors

$$\tilde{\mathbf{u}} := \begin{bmatrix} u(\tilde{\mathbf{x}}_1) \\ \vdots \\ u(\tilde{\mathbf{x}}_n) \end{bmatrix} \quad \text{and} \quad \mathbf{u}_{err} := \begin{bmatrix} u_{err}(\tilde{\mathbf{x}}_1) \\ \vdots \\ u_{err}(\tilde{\mathbf{x}}_n) \end{bmatrix} \tag{3.1.5}$$

so that the error in the solution is given by

$$err := \|\tilde{\mathbf{u}} - \mathbf{u}_{err}\|_2. \tag{3.1.6}$$

### 3.2 First derivative

We now denote the gravitational force $G := \nabla u$, and so a component of $G$ in the direction of a basis vector is given by $G_\alpha = \partial_\alpha u$ with $\alpha = 1, 2$. Applying this derivative to (3.0.1) gives

$$G_\alpha \approx \sum_{j=1}^{n} g_j \partial_\alpha K(\mathbf{x}, \mathbf{y}_j). \tag{3.2.1}$$

We now choose points $\mathbf{x}_i \in \Gamma_0$, $1 \le i \le n$ with components $(x_{i_1}, x_{i_2})$ and points $\mathbf{y}_j \in \partial\Omega$, $1 \le j \le 2n$ (as to maintain a square system), with components $(y_{j_1}, y_{j_2})$. Define the matrices $A_\alpha := [a_{ij}^\alpha]$, $\alpha = 1, 2$, where

$$a_{ij}^\alpha := \partial_\alpha K(\mathbf{x}_i, \mathbf{y}_j) = \frac{x_{i_\alpha} - y_{j_\alpha}}{|\mathbf{x}_i - \mathbf{y}_j|^2}, \tag{3.2.2}$$

and define the vectors

$$\mathbf{g} := \begin{bmatrix} g_1 \\ \vdots \\ g_{2n} \end{bmatrix} \quad \text{and} \quad \mathbf{G}_\alpha := \begin{bmatrix} \partial_\alpha u(\mathbf{x}_1) \\ \vdots \\ \partial_\alpha u(\mathbf{x}_n) \end{bmatrix}. \tag{3.2.3}$$

So the system to solve using both first derivatives becomes

$$A_\alpha \mathbf{g} := \begin{bmatrix} A_1 \\ A_2 \end{bmatrix} \mathbf{g} = \begin{bmatrix} \mathbf{G}_1 \\ \mathbf{G}_2 \end{bmatrix} =: \mathbf{G}. \tag{3.2.4}$$

### 3.3 Second derivative

Choose again $n$ points $\mathbf{x}_i \in \Gamma$ and pick points $\mathbf{y}_j \in \partial\Omega$, $1 \leq j \leq 3n$. Define $A_{\alpha\beta} := [a_{ij}^{\alpha\beta}]$, $\alpha, \beta = 1, 2$. If $\alpha = \beta$ then

$$a_{ij}^{\alpha\beta} := \partial_\alpha^2 K(\mathbf{x}_i, \mathbf{y}_j) = \frac{(x_{i_1} - y_{j_1})^2 + (x_{i_2} - y_{j_2})^2 - 2(x_{i_\alpha} - y_{j_\alpha})^2}{|\mathbf{x}_i - \mathbf{y}_j|^4}. \tag{3.3.1}$$

Otherwise

$$a_{ij}^{\alpha\beta} := \partial_{12} K(\mathbf{x}_i, \mathbf{y}_j) = \frac{-2(x_{i_1} - y_{j_1})(x_{i_2} - y_{j_2})}{|\mathbf{x}_i - \mathbf{y}_j|^4}. \tag{3.3.2}$$

We setup the vectors

$$\mathbf{g} := \begin{bmatrix} g_1 \\ \vdots \\ g_{3n} \end{bmatrix} \quad \text{and} \quad \mathbf{u}_{\alpha\beta} := \begin{bmatrix} \partial_{\alpha\beta}\, u(\mathbf{x}_1) \\ \vdots \\ \partial_{\alpha\beta}\, u(\mathbf{x}_n) \end{bmatrix} \tag{3.3.3}$$

which gives the system

$$A\mathbf{g} := \begin{bmatrix} A_{11} \\ A_{22} \\ A_{12} \end{bmatrix} \mathbf{g} = \begin{bmatrix} \mathbf{u}_{11} \\ \mathbf{u}_{22} \\ \mathbf{u}_{12} \end{bmatrix} =: \mathbf{G}'. \tag{3.3.4}$$

# CHAPTER 4

## Truncated SVD Experiments

The systems discussed above, arising from the measurements on $\Gamma_0$, will be solved using the truncated singular value decomposition (TSVD) method. With this method, the SVD of the matrix $A_{\alpha\beta}$ is computed. The solution is found using only the first $t$ columns of the SVD, where $t$ is known as the truncation level. The solution at each truncation level will be compared with an exact solution calculated using points $\tilde{\mathbf{x}}$ on $\Gamma_{err}$. We want to choose the truncation level where the error is minimized, $t = k_{min(err)}$. This allows us to avoid the small singular values that can degrade the solution in the presence of noise.

### 4.1 Measurements around a circle

#### 4.1.1 Calculations

We start with the plate source $T$ centered at the origin, inside a disk of radius $R$ which is also centered at the origin. Let $s = R\theta$ and $\zeta = Re^{i\theta}$ with $ds = R\,d\theta$. For a point outside the disk $z = re^{i\theta}$, the potential is transformed as follows:

$$\begin{aligned} u(z) &= \int_{|\zeta|=R} \log|z-\zeta|\rho(\zeta)\,ds(\zeta) \\ &= \log|z| \int_{|\zeta|=R} \rho(\zeta)\,ds + \int_{|\zeta|=R} \log|1-\frac{\zeta}{z}|\rho(\zeta)\,ds \\ &= \log|z| \int_0^{2\pi} \rho(Re^{i\theta})R\,d\theta + \mathrm{Re}\left(\int_{|\zeta|=R} \log\left(1-\frac{\zeta}{z}\right)\rho(\zeta)\,ds\right) \\ &= 2\pi R\log|z|\left[\frac{1}{2\pi}\int_0^{2\pi}\rho(Re^{i\theta})\,d\theta\right] - \mathrm{Re}\left(\int_0^{2\pi}\sum_{k=1}^{\infty}\frac{1}{k}\left(\frac{Re^{i\theta}}{z}\right)^k \rho(Re^{i\theta})R\,d\theta\right) \end{aligned} \tag{4.1.1}$$

Let

$$\hat{\rho}_0 = \frac{1}{2\pi}\int_0^{2\pi}\rho(Re^{i\theta})\,d\theta, \tag{4.1.2}$$

so then

$$\begin{aligned} u(z) &= 2\pi R\hat{\rho}_0 \log|z| - \operatorname{Re}\left(\sum_{k=1}^{\infty} \frac{R}{k}\left(\frac{R}{z}\right)^k \int_0^{2\pi} \rho(Re^{i\theta})e^{ik\theta}\, d\theta\right) \\ &= 2\pi R\hat{\rho}_0 \log|z| - \operatorname{Re}\left(\sum_{k=1}^{\infty} \frac{R}{k}\left(\frac{R}{z}\right)^k 2\pi\left[\frac{1}{2\pi}\int_0^{2\pi} \rho(Re^{i\theta})e^{ik\theta}\, d\theta\right]\right). \end{aligned} \tag{4.1.3}$$

Now let

$$\hat{\rho}_{-k} = \frac{1}{2\pi}\int_0^{2\pi} \rho(Re^{i\theta})e^{ik\theta}\, d\theta \tag{4.1.4}$$

and note that since $\rho$ is real, $\overline{\hat{\rho}_{-k}} = \hat{\rho}_k$. Using also the fact $\operatorname{Re}(()\, z) = \frac{1}{2}(z + \overline{z})$,

$$\begin{aligned} u(z) &= 2\pi R\hat{\rho}_0 \log|z| - \operatorname{Re}\left(\sum\right)_{k=1}^{\infty} \frac{2\pi R^{k+1}}{k}\hat{\rho}_{-k}z^{-k} \\ &= 2\pi R\hat{\rho}_0 \log|z| - \sum_{k=1}^{\infty} \frac{\pi R^{k+1}}{k}(\hat{\rho}_{-k}z^{-k} + \overline{\hat{\rho}_{-k}z^{-k}}) \\ &= 2\pi R\hat{\rho}_0 \log|z| - \pi\sum_{k=1}^{\infty} \frac{R^{k+1}}{k}(\hat{\rho}_{-k}z^{-k} + \hat{\rho}_k\overline{z}^{-k}) \\ &= 2\pi R\hat{\rho}_0 \log r - \pi\sum_{k=1}^{\infty} \frac{R^{k+1}}{k}(\hat{\rho}_{-k}r^{-k}e^{-ik\theta} + \hat{\rho}_k r^{-k}e^{ik\theta}) \\ &= 2\pi R\hat{\rho}_0 \log r - \pi\sum_{k=1}^{\infty} \frac{R}{k}\left(\frac{R}{r}\right)^k 2\operatorname{Re}\left(\hat{\rho}_k e^{ik\theta}\right) \\ &= 2\pi R\hat{\rho}_0 \log r - 2\pi\sum_{k=1}^{\infty} \frac{R}{k}\left(\frac{R}{r}\right)^k \operatorname{Re}\left(\hat{\rho}_k e^{ik\theta}\right). \end{aligned} \tag{4.1.5}$$

When we discretize using an even number of $m$ points, then $\left(\frac{R}{r}\right)^m = \left(\frac{R}{r}\right)^{2n} = \left(\left(\frac{R}{r}\right)^n\right)^2$. Thus, we can expect to find spectral accuracy in our solutions. Example 4.1.1 demonstrates this version of our problem and Table 4.1.1 displays the (approximately) spectral errors.

**Example 4.1.1.** Consider a plate source $T$ centered at the origin with length 0.25 and width 0.15. Let $\Omega$ be a circular domain of radius $R = 1$ and $\Gamma_0$ be a circle of radius $r = 1.1$, both centered at the origin. Error is measured on a circle $\Gamma_{err}$ centered at the origin of radius $rerr = 1.2$. Dirichlet data is measured on $\Gamma_0$.

| Msmts | 1E-003 noise | | 1E-006 noise | | 0E+000 noise | |
|---|---|---|---|---|---|---|
| | $\min(err)$ | $k_{\min(err)}$ | $\min(err)$ | $k_{\min(err)}$ | $\min(err)$ | $k_{\min(err)}$ |
| 20 | 2.5812E-002 | 4 | 2.5164E-002 | 37 | 2.5164E-002 | 37 |
| 40 | 2.0647E-003 | 5 | 5.0267E-004 | 12 | 5.0259E-004 | 79 |
| 80 | 1.6856E-003 | 4 | 2.1712E-006 | 13 | 2.3858E-007 | 159 |
| 160 | 5.5813E-004 | 4 | 2.1158E-006 | 12 | 5.7647E-014 | 46 |

Table 4.1.1: Minimum relative error between calculated and actual field at varying noise levels.

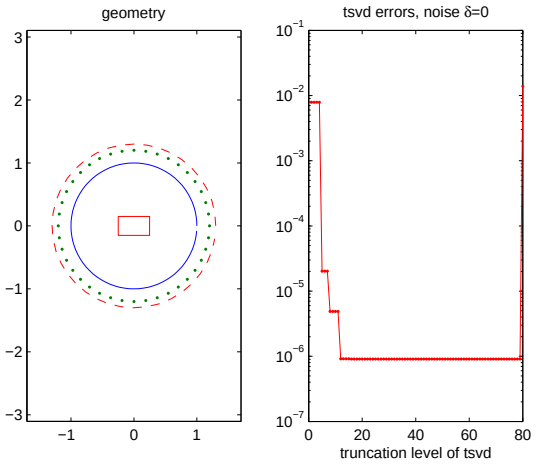


Figure 4.1.1: Plate source at the origin. The dotted circle represents $\Gamma_0$, the solid circle is $\partial\Omega$, and dashed circle is $\Gamma_{err}$.

## 4.2 Measurements along a line segment

### 4.2.1 First derivative (of the potential)

The figures and tables in this section were generated by measuring first derivative (of the potential) data.

**Centered rectangle**

We first examine a plate centered in the unit circle at varying noise levels. The lower left-hand vertex of the rectangle has coordinate (-0.25,-0.15), with a length of 0.5 and a width of 0.3. Let $\Omega$ be a circular domain of radius $R = 1$ and $\Gamma_0$ be a line segment with length 3, both centered at the origin and $r = 2$. Error is measured on a circle $\Gamma_{err}$ centered at the origin of radius $rerr = 1.5$. Figure 4.2.1 shows the geometry along with a graph of the error at varying TSVD truncation levels.

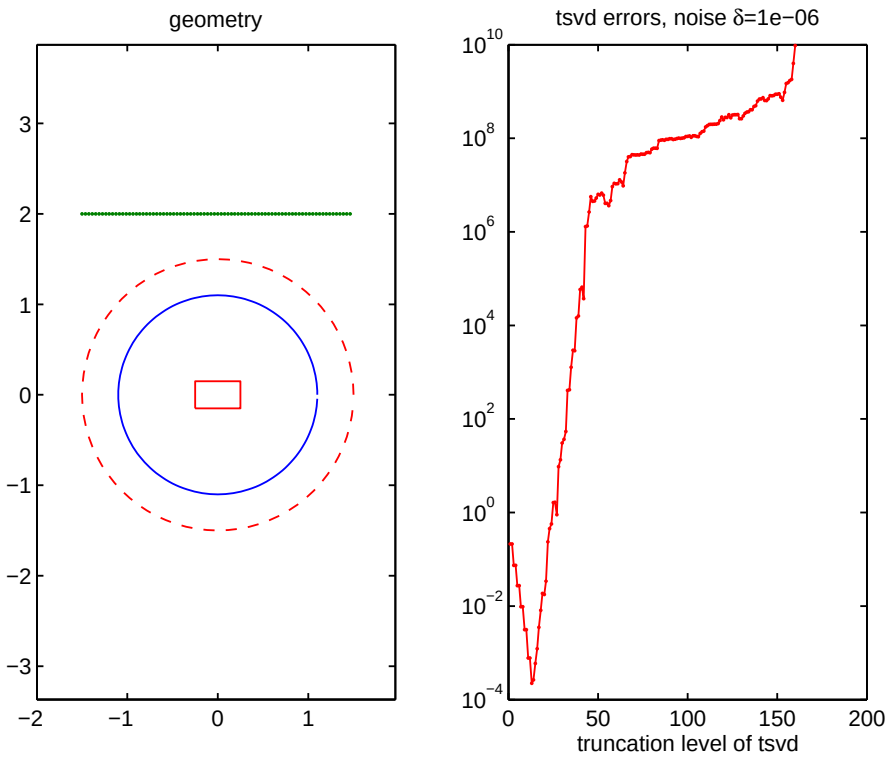


Figure 4.2.1: First derivative data, centered plate source, 80 measurements.

Table 4.2.1 shows minimum error at varying noise levels and number of measurements.

| | 1E-03 noise | | 1E-06 noise | | 0E+00 noise | |
|---|---|---|---|---|---|---|
| Msmts | $\min(err)$ | $k_{\min(err)}$ | $\min(err)$ | $k_{\min(err)}$ | $\min(err)$ | $k_{\min(err)}$ |
| 20 | 7.1764E-03 | 7 | 3.3918E-04 | 13 | 4.2120E-05 | 22 |
| 40 | 9.4227E-03 | 7 | 3.8100E-04 | 13 | 1.5622E-06 | 34 |
| 80 | 7.5912E-03 | 9 | 1.1503E-04 | 13 | 8.0370E-07 | 35 |
| 160 | 5.2870E-03 | 9 | 3.3336E-04 | 17 | 3.9838E-07 | 35 |

Table 4.2.1: Minimum relative error between calculated and actual field at varying noise levels, measurements of the first derivative on a line segment, centered plate.

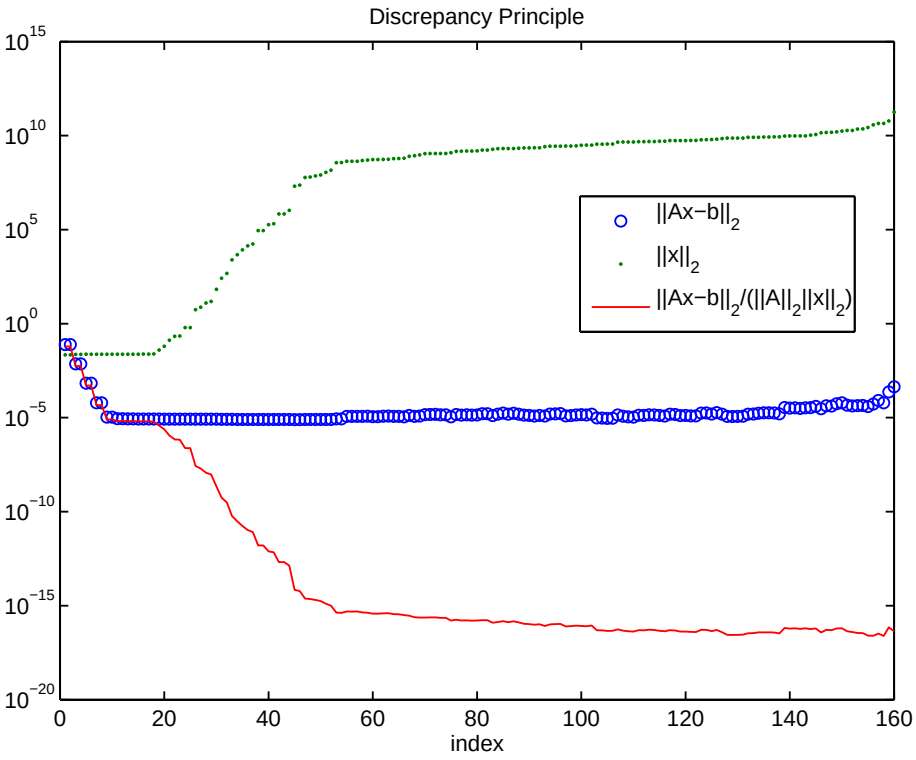


Figure 4.2.2: Comparison of the norm of the residual and the norm of the solution.

### Slightly off-center rectangle

We now move the plate to the right; the lower-left vertex of the rectangle is at (0.25,-0.15). Length and width are the same. Figure 4.2.3 shows this geometry along with TSVD truncation relative errors. Table 4.2.2 shows relative error between the actual and calculated

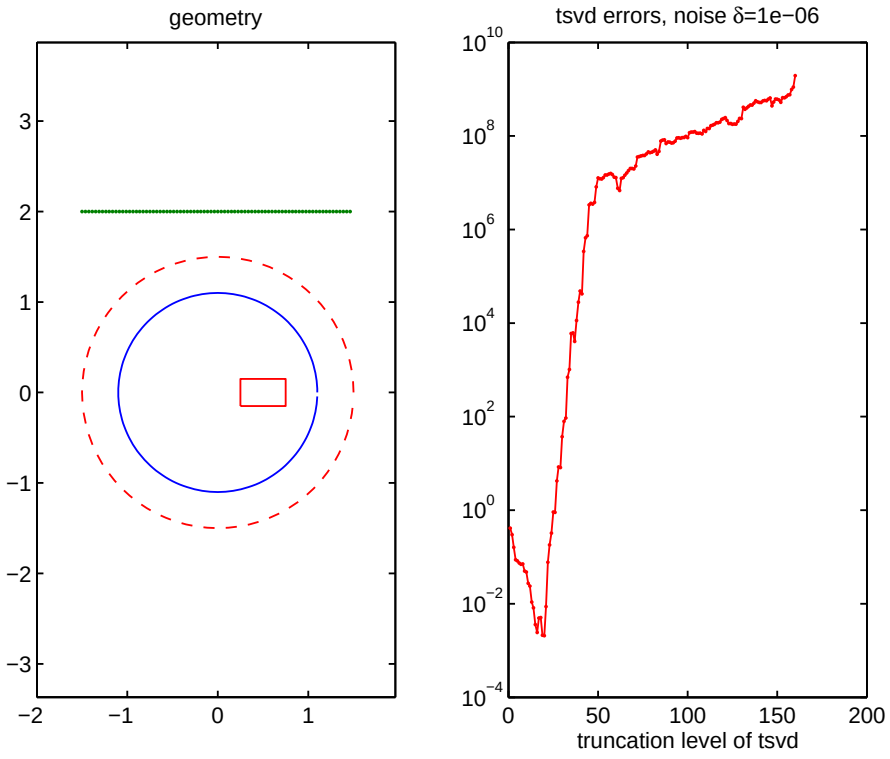


Figure 4.2.3: First derivative data, slightly off-center plate.

fields in this case.

| Msmts | 1E-03 noise | | 1E-06 noise | | 0E+00 noise | |
|---|---|---|---|---|---|---|
| | $\min(err)$ | $k_{\min(err)}$ | $\min(err)$ | $k_{\min(err)}$ | $\min(err)$ | $k_{\min(err)}$ |
| 20 | 3.4379E-02 | 10 | 4.2617E-03 | 17 | 1.2755E-04 | 24 |
| 40 | 5.3634E-02 | 10 | 3.1144E-03 | 15 | 1.9184E-05 | 37 |
| 80 | 4.6589E-02 | 10 | 2.3788E-03 | 16 | 1.4640E-05 | 38 |
| 160 | 4.0545E-02 | 11 | 2.3190E-03 | 18 | 2.8628E-05 | 38 |

Table 4.2.2: Minimum relative error between calculated and actual field at varying noise levels.

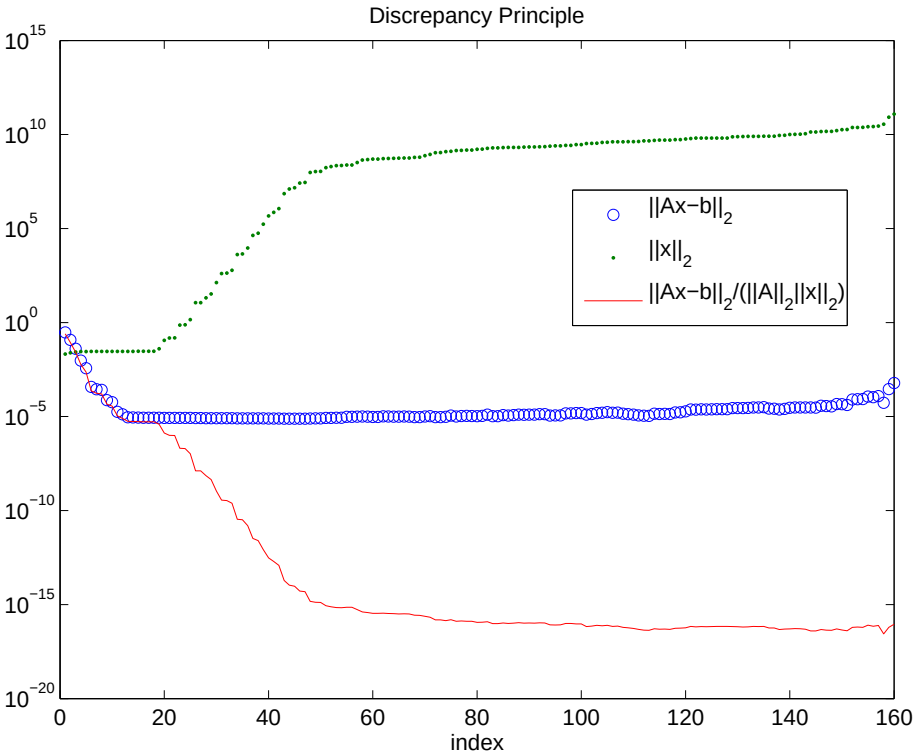


Figure 4.2.4: Comparison of the norm of the residual and the norm of the solution.

### Rectangle on single-layer boundary

The lower-left vertex of the rectangle is now at (0.6,-0.15); it intersects the single-layer boundary. Figure 4.2.5 shows this geometry along with relative errors. Table 4.2.3 shows

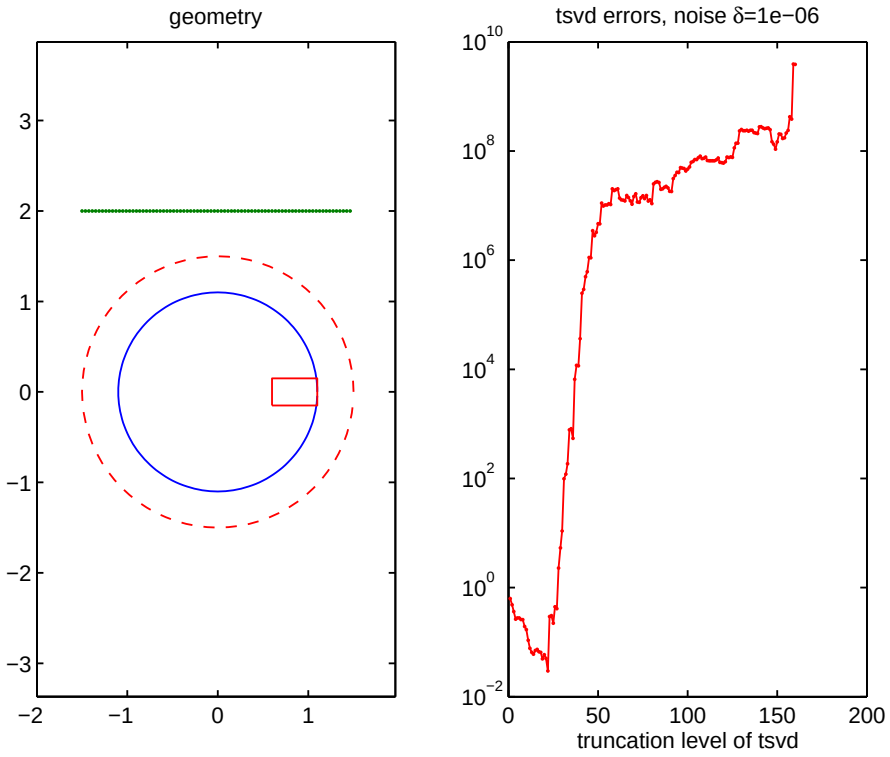


Figure 4.2.5: First derivative data, plate intersects single-layer boundary.

relative error between the actual and calculated fields in this case.

| Msmts | 1E-03 noise | | 1E-06 noise | | 0E+00 noise | |
|---|---|---|---|---|---|---|
| | $\min(err)$ | $k_{\min(err)}$ | $\min(err)$ | $k_{\min(err)}$ | $\min(err)$ | $k_{\min(err)}$ |
| 20 | 7.9353E-02 | 12 | 5.6709E-02 | 14 | 4.0607E-03 | 27 |
| 40 | 8.0863E-02 | 13 | 4.3251E-02 | 20 | 1.2004E-03 | 40 |
| 80 | 6.7031E-02 | 12 | 4.0592E-02 | 21 | 1.1669E-03 | 45 |
| 160 | 6.4260E-02 | 12 | 1.9035E-02 | 21 | 1.2894E-03 | 40 |

Table 4.2.3: Minimum relative error between calculated and actual field at varying noise levels.

### 4.2.2 Second derivative

#### Centered rectangle

Figure 4.2.6 shows the problem geometry along with TSVD truncation relative error. Table 4.2.4 shows relative errors at varying noise levels.

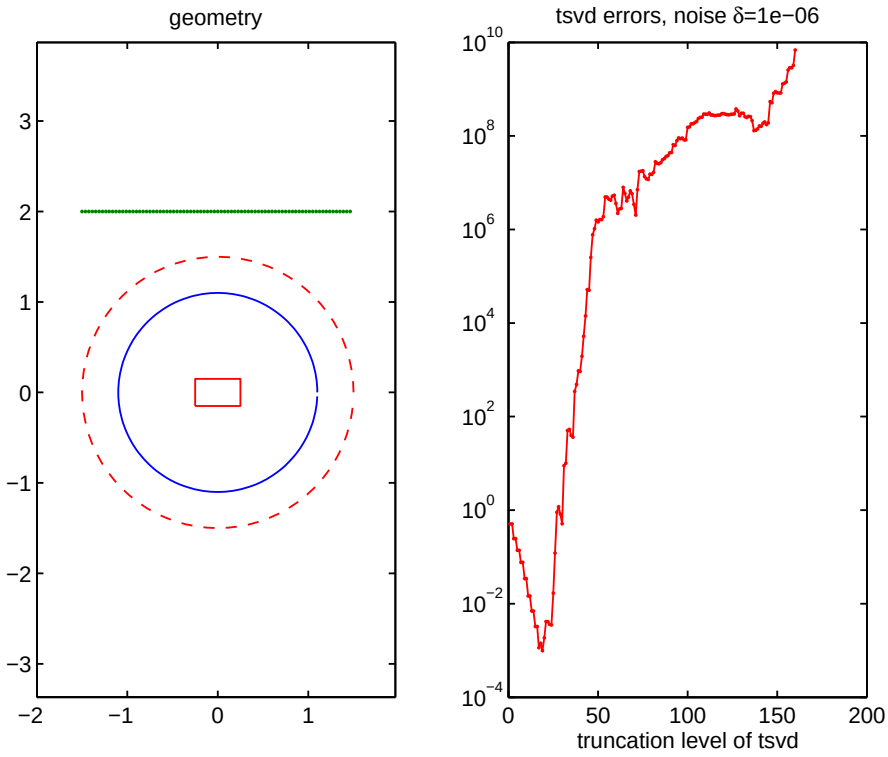


Figure 4.2.6: Second derivative data, centered plate.

#### Slightly off-center rectangle

Figure 4.2.7 shows geometry and relative TSVD errors. Table 4.2.5 shows relative errors.

#### Rectangle on single-layer boundary

More figures here. Table 4.2.6 shows relative errors.

| Msmts | 1E-03 noise | | 1E-06 noise | | 0E+00 noise | |
|---|---|---|---|---|---|---|
| | $\min(err)$ | $k_{\min(err)}$ | $\min(err)$ | $k_{\min(err)}$ | $\min(err)$ | $k_{\min(err)}$ |
| 20 | 1.9940E-02 | 11 | 8.4104E-04 | 17 | 1.0178E-04 | 21 |
| 40 | 2.0283E-02 | 13 | 2.1502E-03 | 17 | 1.0445E-06 | 37 |
| 80 | 2.9879E-02 | 13 | 1.2461E-03 | 17 | 5.4850E-07 | 39 |
| 160 | 2.7465E-02 | 13 | 1.4396E-03 | 17 | 9.8765E-07 | 39 |

Table 4.2.4: Minimum relative error between calculated and actual field at varying noise levels.

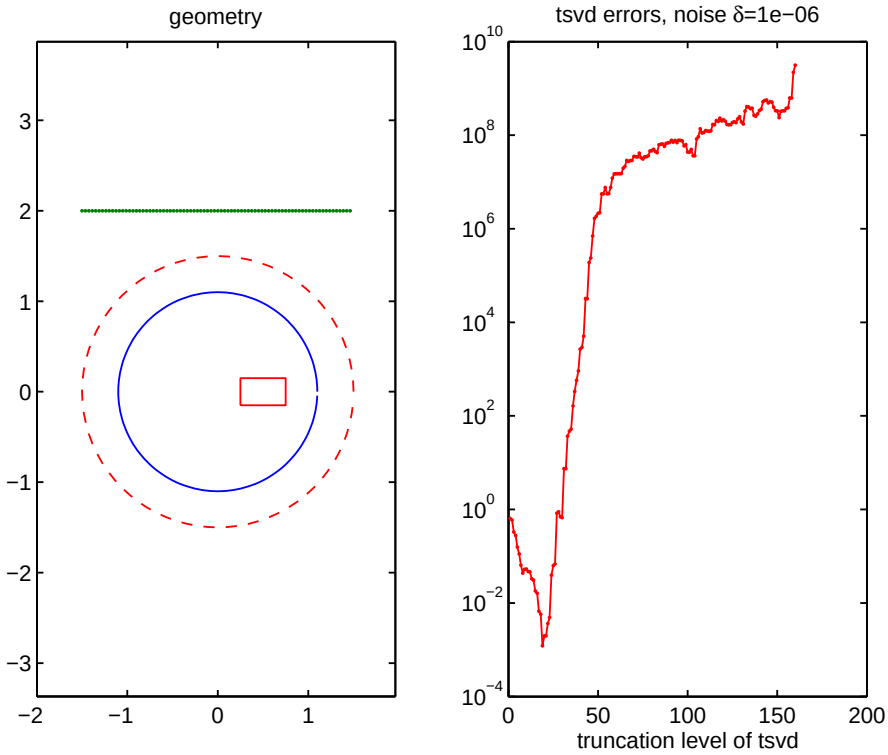


Figure 4.2.7: Second derivative data, plate slightly offset from center.

### 4.2.3 Third derivative

#### Centered rectangle

Figure 4.2.9 shows geometry with errors. Table 4.2.7 shows errors with varying noise.

| Msmts | 1E-03 noise | | 1E-06 noise | | 0E+00 noise | |
|---|---|---|---|---|---|---|
| | $\min(err)$ | $k_{\min(err)}$ | $\min(err)$ | $k_{\min(err)}$ | $\min(err)$ | $k_{\min(err)}$ |
| 20 | 2.7111E-02 | 13 | 4.5047E-03 | 19 | 2.2622E-04 | 23 |
| 40 | 2.8132E-02 | 13 | 2.0862E-03 | 19 | 8.6631E-06 | 41 |
| 80 | 3.7304E-02 | 13 | 3.0140E-03 | 19 | 1.3646E-05 | 42 |
| 160 | 1.8448E-02 | 14 | 1.7980E-03 | 19 | 1.7283E-05 | 40 |

Table 4.2.5: Minimum relative error between calculated and actual field at varying noise levels.

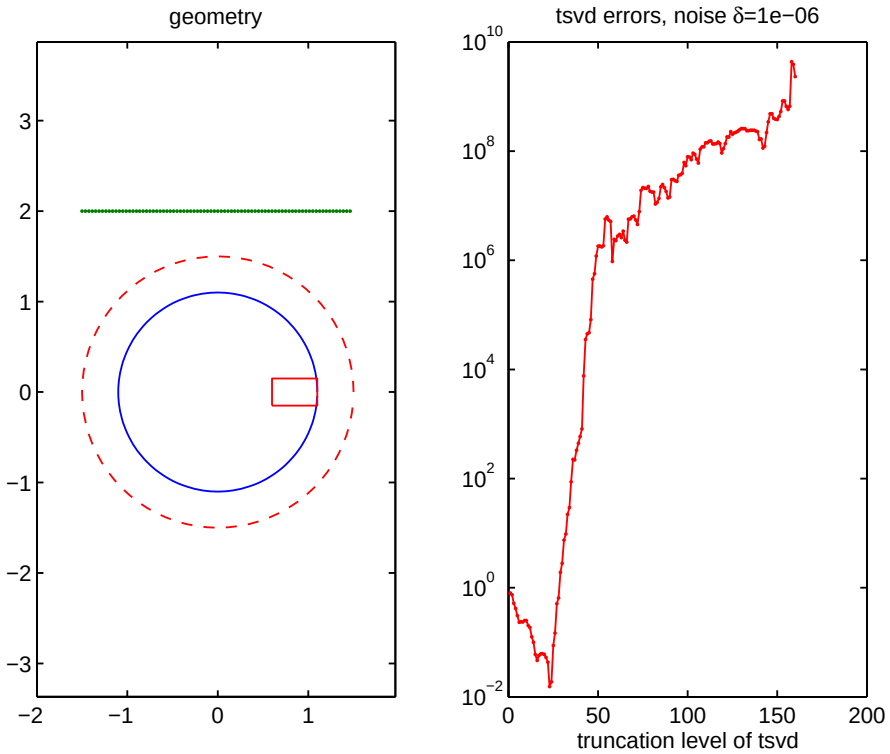


Figure 4.2.8: Second derivative data, plate intersects single-layer boundary.

| Msmts | 1E-03 noise | | 1E-06 noise | | 0E+00 noise | |
|---|---|---|---|---|---|---|
| | $\min(err)$ | $k_{\min(err)}$ | $\min(err)$ | $k_{\min(err)}$ | $\min(err)$ | $k_{\min(err)}$ |
| 20 | 5.4481E-02 | 15 | 3.6816E-02 | 21 | 7.7985E-03 | 25 |
| 40 | 6.5134E-02 | 14 | 4.3148E-02 | 22 | 3.5971E-04 | 45 |
| 80 | 9.0299E-02 | 14 | 1.4788E-02 | 24 | 1.3281E-03 | 44 |
| 160 | 7.8816E-02 | 17 | 2.9683E-02 | 23 | 1.4756E-03 | 44 |

Table 4.2.6: Minimum relative error between calculated and actual field at varying noise levels.

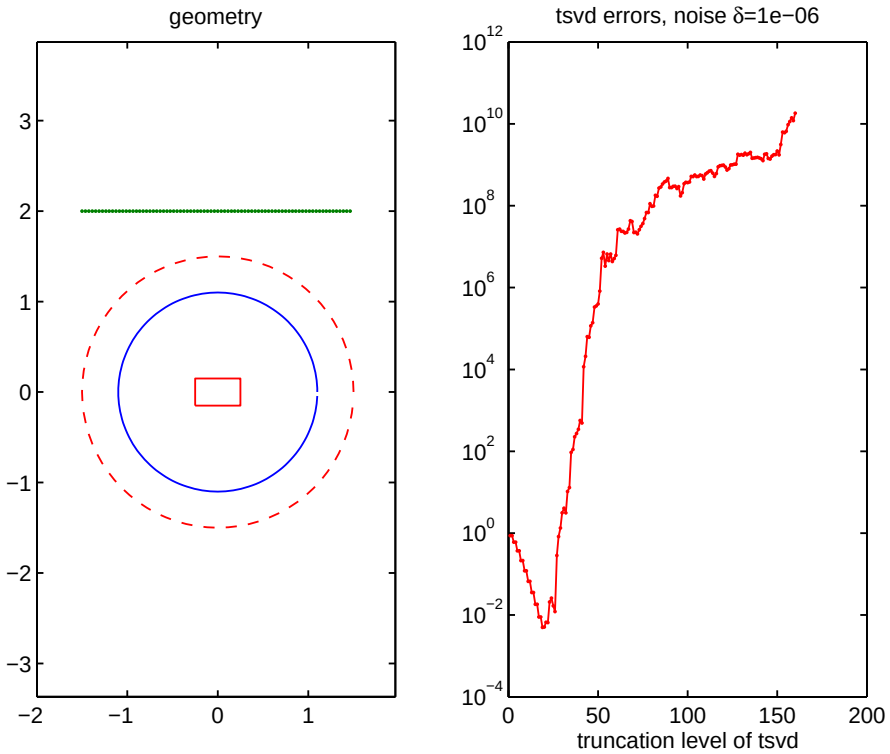


Figure 4.2.9: Third derivative data, centered plate.

| Msmts | 1E-03 noise | | 1E-06 noise | | 0E+00 noise | |
|---|---|---|---|---|---|---|
| | $\min(err)$ | $k_{\min(err)}$ | $\min(err)$ | $k_{\min(err)}$ | $\min(err)$ | $k_{\min(err)}$ |
| 20 | 8.2756E-02 | 13 | 4.1209E-03 | 19 | 6.9354E-04 | 22 |
| 40 | 3.2768E-02 | 16 | 4.5369E-03 | 19 | 7.2474E-07 | 37 |
| 80 | 6.8103E-02 | 11 | 5.8992E-03 | 19 | 4.9501E-07 | 38 |
| 160 | 8.1199E-02 | 11 | 3.9056E-03 | 19 | 5.2013E-07 | 37 |

Table 4.2.7: Minimum relative error between calculated and actual field at varying noise levels.

### Slightly off-center rectangle

Figure 4.2.10 shows geometry with errors. Table 4.2.8 shows errors with varying noise.

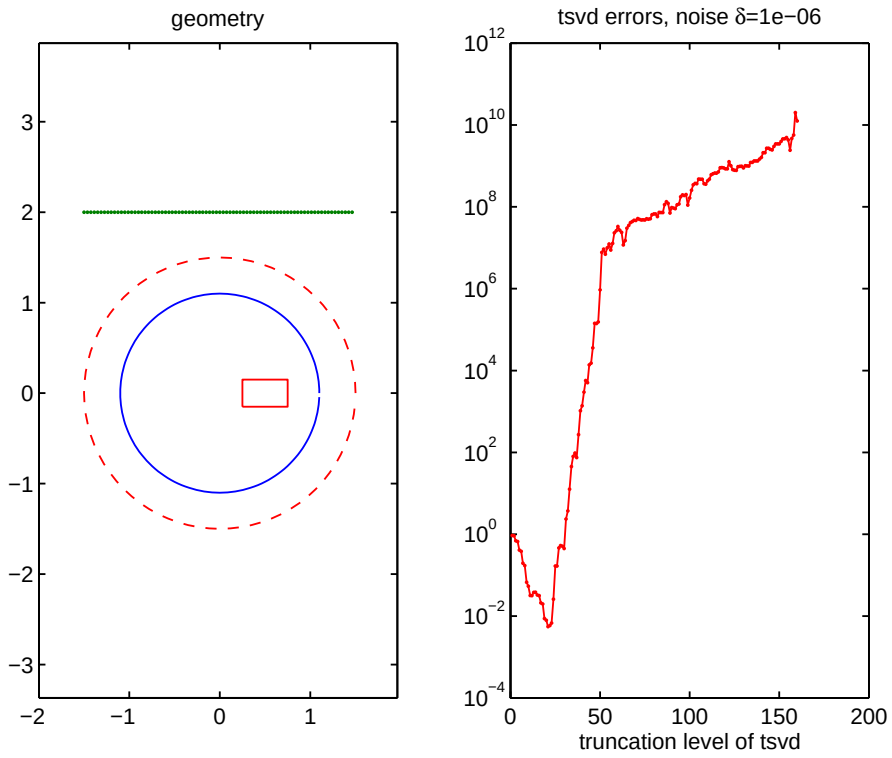


Figure 4.2.10: Third derivative data, plate slightly off-center.

| Msmts | 1E-03 noise | | 1E-06 noise | | 0E+00 noise | |
|---|---|---|---|---|---|---|
| | $\min(err)$ | $k_{\min(err)}$ | $\min(err)$ | $k_{\min(err)}$ | $\min(err)$ | $k_{\min(err)}$ |
| 20 | 3.0223E-02 | 11 | 1.0359E-02 | 19 | 4.6922E-04 | 22 |
| 40 | 2.9950E-02 | 11 | 6.9134E-03 | 21 | 5.3327E-06 | 41 |
| 80 | 3.8208E-02 | 11 | 8.5227E-03 | 21 | 1.0676E-05 | 44 |
| 160 | 4.8255E-02 | 12 | 1.9362E-03 | 21 | 8.3386E-06 | 46 |

Table 4.2.8: Minimum relative error between calculated and actual field at varying noise levels.

### Rectangle on single-layer boundary

Figure 4.2.10 shows geometry with errors. Table 4.2.9 shows errors with varying noise.

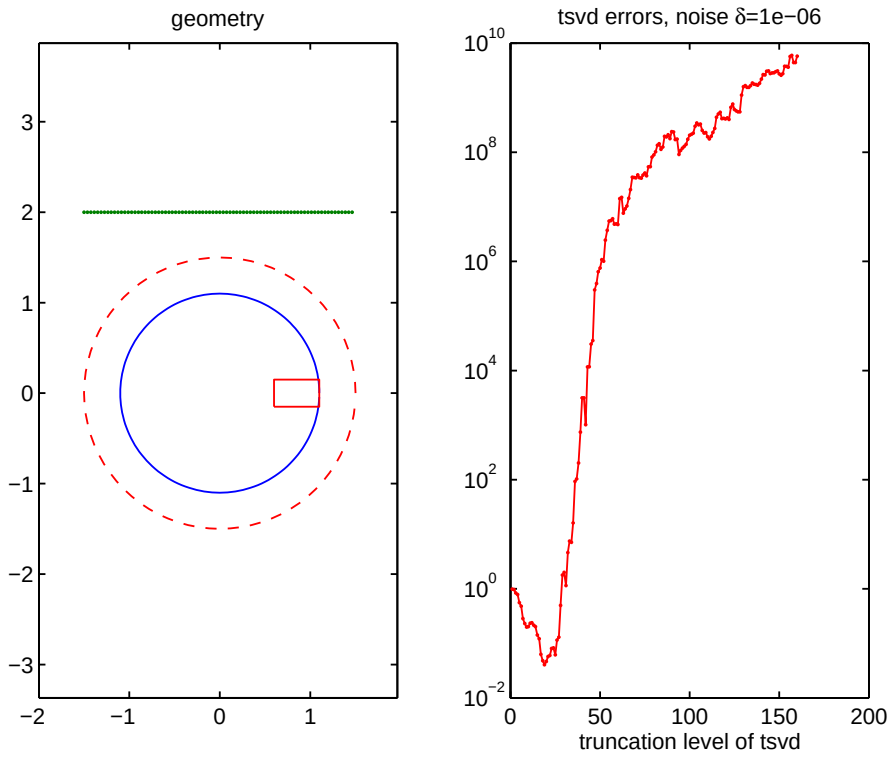


Figure 4.2.11: Third derivative data, plate intersecting single-layer boundary.

| Msmts | 1E-03 noise | | 1E-06 noise | | 0E+00 noise | |
|---|---|---|---|---|---|---|
| | $\min(err)$ | $k_{\min(err)}$ | $\min(err)$ | $k_{\min(err)}$ | $\min(err)$ | $k_{\min(err)}$ |
| 20 | 9.8639E-02 | 16 | 2.5488E-02 | 21 | 8.4783E-03 | 25 |
| 40 | 1.4833E-01 | 16 | 1.4276E-02 | 25 | 1.3555E-03 | 45 |
| 80 | 1.9848E-01 | 9 | 3.7321E-02 | 24 | 9.5787E-04 | 46 |
| 160 | 6.9255E-02 | 15 | 3.8432E-02 | 23 | 9.7444E-04 | 46 |

Table 4.2.9: Minimum relative error between calculated and actual field at varying noise levels.

# CHAPTER 5

## Center of Gravity

### 5.1 Theory

Let $D$ be an open bounded set, $D \subset \Omega \subset \mathbb{R}^n$ where $\Omega$ is given and open. We will assume that $D$ is convex, $\mu$ is zero outside $\bar{D}$, and that $\mu$ is a characteristic function of $D$, $\mu = \chi_D$. The center of gravity of $D$ is the point

$$\mathbf{Q} = \|\mu\|^{-1} \int_D x dD. \tag{5.1.1}$$

Recall that the gravitational potential generated by the mass distribution function $\mu$ is given by

$$U(\mathbf{x}; \mu) = \int K(\mathbf{x}, \mathbf{y}) d\mu(\mathbf{y}), \tag{5.1.2}$$

where

$$K(\mathbf{x}, \mathbf{y}) = \begin{cases} -\frac{1}{2\pi} \ln |\mathbf{x} - \mathbf{y}|, & n = 2, \\ 1/4\pi |\mathbf{x} - \mathbf{y}|, & n = 3. \end{cases} \tag{5.1.3}$$

**Theorem 5.1.1.** *Orthogonality Relations. Let $-\Delta U = \mu$ near $\overline{\Omega}$, $\mu \in L^p(\Omega)$, $\mu = 0$ on $\Omega^+$. Then*

$$\int_\Omega \mu v = \int_{\partial\Omega} (\partial_\nu v U - \partial_\nu U v) \tag{5.1.4}$$

*for any solution $v$ to the equation $\Delta v = 0$ near $\overline{\Omega}$.*

*Proof.* The proof of this theorem can be found in [1]. □

**Theorem 5.1.2.** *Suppose we have two measures, $\mu_1$ and $\mu_2$, such that supp$\mu_1, \mu_2 \subset \Omega$. Also, let $U(; \mu_1) = U(; \mu_2)$ on $\Omega^+$. Then*

$$\int_{\partial\Omega} v d\mu_1 = \int_{\partial\Omega} v \mu_2. \tag{5.1.5}$$

*In other words, all moments are equal.*

*Proof.* This follows from Theorem 1.2.9. □

**Corollary 5.1.1.** Suppose we have two measures, $\mu_1$ and $\mu_2$, such that supp$\mu_1, \mu_2 \subset \Omega$. Also, let $U(;\mu_1) = U(;\mu_2)$ on $\Omega^+$. Then the two measures $\mu_1$ and $\mu_2$ have the same centers of gravity.

Since $\mu = \chi_D$ we can write 5.1.4 as

$$\int_D v = \int_{\partial\Omega} (\partial_\nu v U - \partial_\nu U v). \tag{5.1.6}$$

We can let $v = 1$ to have

$$\|\mu\| = \int_D dD = -\int_{\partial\Omega} (\partial_\nu U) \tag{5.1.7}$$

and then take $v = x$ to get

$$\int_D x dD = \int_{\partial\Omega} (\partial_\nu v U - \partial_\nu x U). \tag{5.1.8}$$

Thus, we can write the center of gravity as

$$\mathbf{Q} = \frac{-1}{\int_{\partial\Omega}(\partial_\nu U)} \int_{\partial\Omega} (\partial_\nu v U - \partial_\nu U x). \tag{5.1.9}$$

From Theorem 5.1.2 and Corollary 5.1.1 these integrals can be written in terms of our density function $g$ to get

$$\int_{\partial\Omega} (\partial_\nu U) = -\int_{\partial\Omega} (g d\Gamma) \tag{5.1.10}$$

and

$$\int_{\partial\Omega} (\partial_\nu v U - \partial_\nu U x) = \int_{\partial\Omega} (\partial_\nu x g). \tag{5.1.11}$$

## 5.2 Numerical Results

We assume $\Omega \subset \mathbb{R}^2$ and use the mass densities obtained in Chapter 4. Discretizing to find the total mass $M$ on $\partial\Omega$ we have

$$M = \int_{\partial\Omega} (g d\Gamma) \approx \sum_{i=1}^{n} g_i. \tag{5.2.1}$$

Also, the moments about the $x$- and $y$-axis can be written as

$$M_x \approx R \sum_{i=1}^{n} g_i cos\theta_i \tag{5.2.2}$$

and

$$M_y \approx R \sum_{i=1}^{n} g_i sin\theta_i. \tag{5.2.3}$$

Then we calculate the center of gravity $\mathbf{Q}$ as

$$\mathbf{Q} = (\frac{M_y}{M}, \frac{M_x}{M}). \tag{5.2.4}$$

Multiple experiments were performed using this method. Sample results from first derivative data with 40 measurement points and second derivative data with 80 points are given. As seen in Figures 5.2.1 and 5.2.2 this method places $\mathbf{Q}$ in the target region.

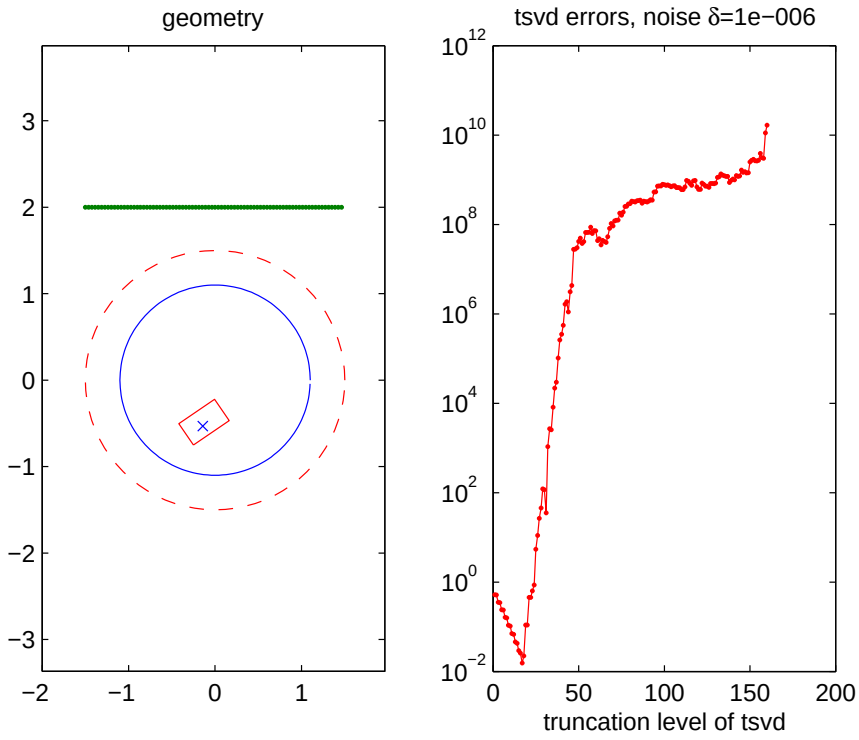


Figure 5.2.1: The mass densities calulated with 80 data points and first derivative data. The marker x shows the center of gravity.

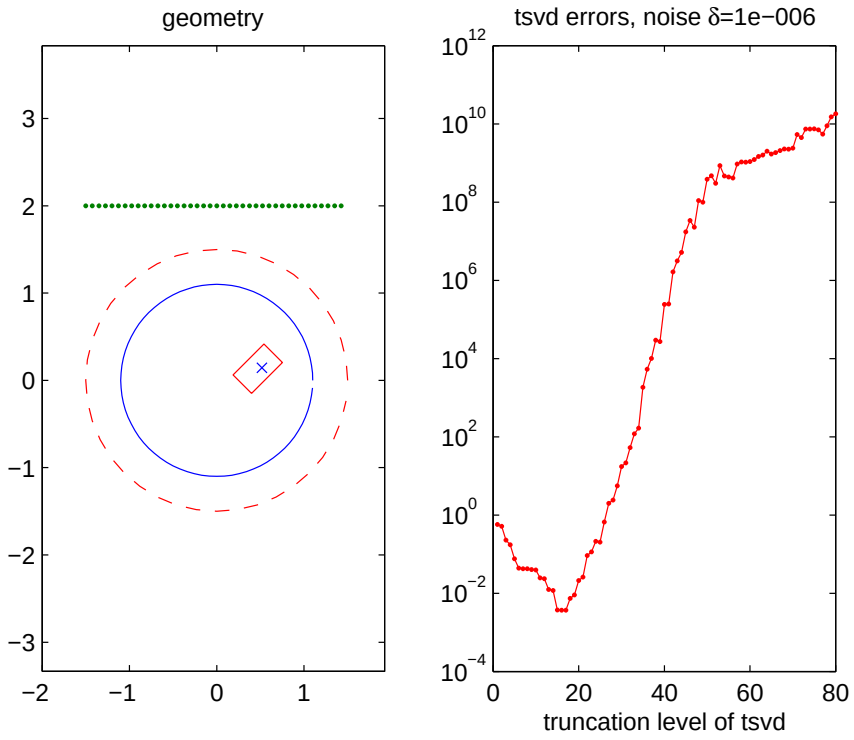


Figure 5.2.2: The mass densities calulated with 40 data points and second derivative data. The marker x shows the center of gravity.

# REFERENCES

## LIST OF REFERENCES

[1] Victor Isakov. *Inverse Source Problems*, volume 34 of *Mathematical Surveys and Monographs*. AMS, Rhode Island, 1990.

[2] Victor Isakov. *Inverse Problems for Partial Differential Equations*, volume 127 of *Applied Mathematical Sciences*. Springer, New York, 1998.

[3] Rainer Kress. *Linear Integral Equations*, volume 82. Springer-Verlag, New York, 1999.